Aerosol Science & Technology

ISSN: 0278-6826 (Print) 1521-7388 (Online) Journal homepage: www.tandfonline.com/journals/uast20

Development of an Atmospheric Particle Dry Deposition Model

Kenneth E. Noll, Msafiri M. Jackson & Ali K. Oskouie

To cite this article: Kenneth E. Noll, Msafiri M. Jackson & Ali K. Oskouie (2001) Development of an Atmospheric Particle Dry Deposition Model, Aerosol Science & Technology, 35:2, 627-636, DOI: 10.1080/02786820119835

To link to this article: https://doi.org/10.1080/02786820119835

Aerosol Science and Technology 35: 627–636 (2001)

Published by Taylor and Francis
0278-6826/01/$12.00 + .00

Development of an Atmospheric Particle Dry Deposition Model

Kenneth E. Noll,[1] Msafiri M. Jackson,[1] and Ali K. Oskouie[1,2]
[1] *Department of Chemical and Environmental Engineering, Illinois Institute of Technology, Chicago, Illinois*
[2] *Metropolitan Water Reclamation, District of Greater Chicago, Chicago, Illinois*

A model to predict the atmospheric dry deposition velocities of particles has been developed that is similar to a model developed for the prediction of particle deposition velocities in vertical pipes. The model correlates the particle deposition velocity (V_d) with Stokes settling velocity (V_{st}), friction velocity (V^*), dimensionless inertial deposition velocity (V_{di}^+), and dimensionless Brownian diffusion deposition velocity (V_{dd}^+). V_{di}^+ is a function of flow Reynolds number (Re) and dimensionless relaxation time (τ^+), while V_{dd}^+ is a function of Schmidt number (Sc). The atmospheric particle mass size distribution and dry deposition flux measured simultaneously with a wide range aerosol classifier (WRAC) and a smooth greased surface were used to calculate V_d and V_{di}^+. The relationship between V_{di}^+, Re, and τ^+ for particles between 1 and 100 μm in diameter was determined using the least square method to obtain coefficients for a sigmoid curve. A sensitivity analysis of the model revealed three distinct particle size ranges: for $\tau^+ > 0.2$ and aerodynamic diameter (d_{pa}) > 8 μm, the controlling parameter is τ^+; for $0.005 < \tau^+ < 0.2$ ($1 < d_{pa} < 8$ μm), the controlling parameters are τ^+ and Re; and for $\tau^+ < 0.005$ ($d_{pa} < 1$ μm), the controlling parameters are Sc and Re. The model was evaluated by determining the ratio between the average calculated flux and the flux measured with a smooth surrogate surface. The new model was found to better fit the experimental data (ratio 1.05 ± 0.45) than the Sehmel–Hodgson model (0.34 ± 0.18), which is often used to predict particle deposition velocities.

A sensitivity analysis for the ambient model revealed three size ranges of model application based on particle diameter. Of the three physical parameters (τ^+, Re, Sc) used in the model, not more than two parameters control the deposition in any one of these size ranges. Based on this analysis, a reduced deposition model for $d_{pa} > 8$ μm, which is a function of V_{st}, V^*, τ^+, has been developed.

INTRODUCTION

Atmospheric particles are deposited by several processes, including eddy diffusion, Brownian diffusion, inertial effects, and gravity settling. Sehmel (1970, 1971, and 1973) proposed that the particle transport process could be described solely by an effective diffusivity, which couples the effects of inertial, and eddy diffusion. The turbulent burst theory, which is often used to explain particle deposition, is based on observations that fluid motion into the region near the collecting surface occurs via high speed perturbations and that fluid motion out of the region occurs by much slower transport (Kline et al. 1967). Owen (1969) and Liu and Agarwal (1974) proposed that particles in the fluid were transported by convection from the main stream into the region near the wall by the high-speed turbulent bursts. Outside this region, the particles are transported by turbulent diffusion. For particles larger than 1 μm in diameter, the predominant deposition mechanism in a vertical pipe has been shown to be particle inertia (Liu and Agarwal 1974). Recently, Muyshondt et al. (1996) have shown that the particle dimensionless deposition velocity in a vertical tube is a function of flow Reynolds number (Re) and the dimensionless relaxation time (τ^+).

Experimentally determined dry deposition velocities for atmospheric particles in the size range of 5–80 μm in diameter are greater than predictions made with an existing deposition model based on wind tunnel experiments (Sehmel and Hodgson 1978), particularly at higher wind speeds (Noll and Fang 1989; Lin et al. 1994). In this paper a deposition velocity model will be developed using a least square procedure to fit a sigmoid curve to ambient data. This model is similar to one developed for deposition in a vertical pipe (Muyshondt et al. 1996). The pipe flow model was applied to atmospheric conditions because the mechanisms controlling deposition in turbulent flow in pipes and the atmosphere are similar. However, different scaling factors (incorporated in the Reynolds' number term) are required for characterization of pipe and atmospheric particle deposition. The model is based on 20 atmospheric samples collected at flow Reynolds numbers ranging from 9,000 to 30,000. The incorporation of inertial effects via a flow Reynolds number and dimensionless relaxation time improves the predictive ability of the model, particularly in the atmospheric particle size range of 1–80 μm.

Received 10 March 1998; accepted 7 June 2000.
Address correspondence to Kenneth E. Noll, Perlstein Hall, Department of Chemical and Environmental Engineering, Illinois Institute of Technology, 10 w 33rd Street, Chicago, IL 60616-3793.

DRY DEPOSITION MODELS

Atmospheric Deposition

There are currently a number of models for predicting dry deposition velocities that can be used in conjunction with measured atmospheric particle concentrations or particle size distributions to calculate dry deposition flux. Many of these models are based either on wind tunnel experiments (Sehmel 1971; Sehmel and Hodgson 1978; McCready 1986) or have been theoretically derived from assumed deposition mechanisms (Slinn and Slinn 1980; Peters and Eiden 1992; Wu et al. 1992).

Particle deposition in the atmosphere has been described by a one-dimensional steady continuity equation for the deposition flux (N) (Friedlander and Johnstone 1957).

$$N = -(\varepsilon + D)\frac{dC}{dz} - V_t C, \qquad [1]$$

in which ε is the particle eddy diffusivity, C is the airborne particle concentration, z is the height above the deposition surface, V_t is the particle terminal settling velocity, and Brownian diffusivity (D) is given by

$$D = \frac{\kappa T C_c}{3\pi\mu d_{pa}}, \qquad [2]$$

where κ is the Boltzmann's constant (1.3×10^{-23} J/K) and T is the absolute temperature.

From the integration of the continuity equation (Equation (1)), the deposition velocity (V_d) of particles deposited to a floor surface is

$$V_d = \frac{(-N)}{C_z} = \frac{V_t}{1 - \exp\left(\frac{V_t}{V^*}\mathrm{INT}\right)}, \qquad [3]$$

where C_z is the concentration at a height above deposition surface and INT is the resistance integral that is a function of the dimensionless eddy and Brownian diffusivity for a particle depositing from the reference concentration height to the deposition surface. The integral INT can be subdivided into three components (Sehmel and Hodgson 1978) as follows:

$$\begin{aligned}\mathrm{INT} &= \int_{z^+\,at\,C_z}^{r^+} \frac{dz^+}{\varepsilon/\nu + D/\nu} \\ &= \mathrm{INT}_1 + \mathrm{INT}_2 + \mathrm{INT}_3 \\ &= \int_{z^+\,at\,C_z}^{z^+_{(1-2)}} \frac{dz^+}{\varepsilon/\nu + D/\nu} + \int_{z^+_{(1-2)}}^{z^+_{(2-3)}} \frac{dz^+}{\varepsilon/\nu + D/\nu} + \mathrm{INT}_3, \end{aligned} \qquad [4]$$

where ν is the kinematics viscosity of air and $z^+ = zV^*/\nu$ is the dimensionless distance above the surface. The integration limits were (1) particle concentration, C_z, at a reference height, z, and (2) a particle concentration of zero at the dimensionless particle radius, r^+, from the deposition surface. Surface integral resistance, INT_3, was evaluated with least square techniques of Sehmel and Hodgson using wind tunnel data as follows:

$$\begin{aligned}\mathrm{INT}_3 = -\exp\Big\{&-378.051 + 16.498\ln(\mathrm{Sc}) \\ &+ [\ln(\tau^+)]\Big[-11.818 - 0.2863\ln\tau^+ \\ &+ 0.3226\left(\ln\left(\frac{d_{pa}}{Z_o}\right)\right) - 0.3385\ln\left(\frac{D}{Z_o V^*}\right)\Big] \\ &- 12.804\ln(d)\Big\}, \end{aligned} \qquad [5]$$

where Sc is Schmidt number (i.e., $\mathrm{Sc} = D/\nu$) and Z_o is surface roughness height. Reynolds' number is not a parameter in this model.

Deposition in Vertical Pipes

The diffusion of particles toward the wall in vertical pipes is due to the radial component of turbulence. Early researchers modeled this process by assuming that the particle diffusivity was a function of the fluid momentum diffusivity (Friedlander and Johnstone 1957; Liu and Ilori 1974). Tennekes and Lumley (1982) demonstrated that turbulent diffusion was a function of the flow Reynolds number.

The fundamental controlling deposition in turbulent flow in pipes and the atmosphere are similar. Using vertical pipe deposition data, Muyshondt et al. (1996) demonstrated that dimensionless deposition velocity is a function of dimensionless relaxation time and Reynolds number. Dimensionless inertial deposition velocity, V_{di}^+, was correlated with flow Reynolds number (Re) and dimensionless relaxation time (τ^+) in the form of a sigmoid curve as follows:

$$V_{d1}^+ = a_1 e^{-0.5\{(\mathrm{Re}-a_2)/a_3\}^2} + a_4 e^{-0.5\{(\ln_\tau^+ - \ln a_5)/a_6\}^2}, \qquad [6]$$

where Re is the flow Reynolds number (i.e., $\mathrm{Re} = UL/\nu$, where L is the characteristic length (in this case the pipe diameter, 1.3–10.2 cm), U is fluid velocity, and ν is the kinematics viscosity). The dimensionless relaxation time, τ^+, is defined as

$$\tau^+ = \frac{\tau V^{*2}}{\nu}, \qquad [7]$$

where V^* is the friction velocity and τ is the particle relaxation time defined as

$$\tau = \frac{C_c \rho_p {d_{pa}}^2}{18\mu}, \qquad [8]$$

where C_c is the Cunningham slip correction factor, ρ_p is the particle density, d_{pa} is the particle aerodynamic diameter, and μ is the absolute viscosity of the fluid. The resulting coefficients (Equation (6)) fit by a least square technique were

$$\begin{aligned} a_1 &= 0.0226, \quad a_2 = 40300, \quad a_3 = 15330, \\ a_4 &= 0.1394, \quad a_5 = 49.0, \quad a_6 = 1.136. \end{aligned}$$

Equation (6) essentially represents a surface in three-dimensional space. The aerodynamic particle diameters ranged from 5 to 20 μm. The correlation coefficient, r^2, of Equation (6) with the experimental pipe data was 0.983 (Muyshondt et al. 1996). The Reynolds number range in the experiments was between 9,000–30,000.

MATERIAL AND METHODS

Atmospheric Particle Dry Deposition

The deposition plate used in this study has been used previously in ambient flux measurements (Holsen and Noll 1992; Lin et al. 1993) and is similar to those used in wind tunnel studies (McCready 1986). It was made of polyvinyl chloride (PVC) and is 16 cm long, 7.6 cm wide, and 0.55 cm thick with a sharp leading edge ($<10^\circ$ angle) that is pointed into the wind by wind vane. Mylar strips 7.6 cm long and 2.5 cm wide were used as collection surfaces on the top of the deposition plate. The strips were weighed before and after exposure to determine the mass of particles collected.

Ambient Particle Concentrations and Mass-Size Distribution

The experimental methods used in this study to determine complete atmospheric particle size distributions have been described previously (Lin et al. 1993) and will be briefly summarized here. Atmospheric particle concentrations were measured with a wide range aerosol classifier (WRAC) that uses an Andersen (1 actual cubic foot per minute [ACFM]) nonviable ambient particle sizing sampler (AAPSS) with a preseparator and Noll rotary impactor (NRI). The AAPSS (Graseby Andersen Instruments 1985) is a multistage, multiorifice cascade impactor. The AAPSS collects particles and separates them into the following aerodynamic size intervals: <0.43, 0.43–0.65, 0.65–1.1, 1.1–3.3, 3.3–4.7, 4.7–9.0, 9.0–10.0, and >10 μm (preseparator). The NRI is ideally suited to collect the coarse particles that conventional samplers exclude. It is a multistage rotary inertial impactor that collects large particles by simultaneously rotating four rectangular collectors (stages) of different dimensions through the air (Noll and Fang 1986). In this study, the NRI was operated at 320 rpm to produce theoretical aerodynamic cut diameters of 6.5, 11.5, 24.7, and 36.5 μm for the four stages. All stages of the AAPSS and NRI were covered with greased Mylar films to minimize particle bounce. Also, grease was used to minimize the reentrainment of the collected deposits.

Numerous field studies have been conducted in urban and remote areas using the two sampling methods in combination to characterize the fine and coarse size distributions simultaneously and to compare to dry deposition flux (Lin et al. 1994). Some of the particle sizes collected with the NRI overlap particle sizes collected with the Anderson impactor. The NRI data was comparable to the impactor data in the overlap size range. In this study the size distributions have been shown to be statistically the same in all size ranges (Lin et al. 1994). The overlap cut-sizes are 9.9, 11.5 μm (Cascade) and 6.2, 6.5 μm (NRI), respectively.

Sampling Program

Four sampling campaigns were conducted at Chicago, IL. The samples were collected on the roof of a four-story building (12 m height) located in a mixed institutional, commercial, and residential area on the south of Chicago. The building is located on the Illinois Institute of Technology (IIT) campus, which is located 5.6 km south of Chicago's center and 1.6 km west of Lake Michigan. The IIT campus consists of predominately low-rise buildings, landscaped areas, and asphalt parking lots. Atmospheric samples collected in the first campaign (1992) in Chicago (Table 1) were used for model development, evaluation, and application. Data from the other three Chicago campaigns (Table 2) were used for model evaluation and application. Table 3 summarizes the data. Sampling times for the first campaign (1992) ranged from 4 to 16 h (short term), while for the other three campaigns (1994 and 1995) it ranged from 19 to 86 h (long term).

Data Evaluations

Chamberlain (1960) defined deposition flux (F) as the product of airborn particle concentration (C) and the dry deposition velocity (V_d):

$$F = CV_d. \quad [9]$$

Lin et al. (1993) used a WRAC to measure the ambient particulate concentration (C_I; I denotes particle size interval) in 10 size ranges (0.1–100 μm) and applied a multistep calculation method based on the Chamberlain Equation to determine dry deposition flux (F) as the sum of the individual flux measured in different size interval (F_I):

$$F = \Sigma F_I = \Sigma C_I V_d(d_{pa}, I), \quad [10]$$

where C_I is the particle mass concentration measured by each WRAC stage and $V_d(d_{pa}, I)$ is the deposition velocity for each WRAC stage. Based on the size interval of the WRAC, the deposition velocity (V_{di}) was obtained as

$$V_d(d_{\text{pa}}, I) = \frac{F_I}{C_I}, \quad [11]$$

where F_I was measured using a smooth, greased surface (flat plate) with a sharp leading edge. Particles collected on the deposition plate were counted using an optical microscope with an image processing system (Olympus 1990) to obtain the size and mass distributions of deposited particles (F_I). Figure 1 provides an example of the deposition velocities derived from the measured ambient particle concentration and count converted mass deposition data.

Particles deposited on the deposition plate were counted using $\times$100 and $\times$400 magnifications with an optical microscope and an image analysis processing system. Particles were grouped into fifteen successive size ranges: <0.43, 0.43–0.65, 0.65–1.1, 1.1–2.5, 2.5–3.3, 3.3–4.7, 4.7–5.8, 5.8–6.5, 6.5–11.5,

Table 1
Measured data for 1992 Chicago samples (20 samples used for model development)

Sample ID	Sampling time: Day/night	Sampling time: Period (min)	Avg. wind speed (m/s)	Average temperature (C)	Deposition flux (mg/m^2-day)	Avg. wind direction
4/27/92	D	515	7.6	6.1	241.9	Lake
4/28/92	D	504	4.0	13.0	181.4	Land
4/30/92	D	518	5.0	11.9	164.2	Lake
5/02/92	D	336	7.7	24.0	820.8	Land
5/02/92	N	920	6.0	15.2	466.6	Land
5/07/92	D	528	4.1	19.1	250.6	Lake
5/13/92	D	485	7.4	14.0	665.3	Lake
5/16/92	D	471	7.7	29.4	1356.5	Land
5/20/92	D	518	5.5	26.1	604.8	Lake
5/27/92	D	486	5.4	16.0	129.6	Lake
6/02/92	D	531	4.5	21.7	319.7	Lake
6/08/92	N	884	4.9	17.3	86.4	Lake
6/10/92	D	512	3.9	24.3	371.5	Lake
6/14/92	D	511	4.8	27.7	475.2	Land
6/18/92	N	960	5.9	17.9	259.2	Land
6/18/92	N	880	3.7	15.7	164.2	Lake
6/28/92	D	485	3.5	25.6	233.3	Land
7/07/92	D	260	6.2	24.2	457.9	Land
7/17/92	D	574	6.2	25.3	302.4	Land
8/17/92	N	740	4.2	18.5	224.6	Land
8/21/92	D	568	3.3	26.1	354.2	Land
8/23/92	D	585	5.1	28.2	362.9	Land
8/25/92	D	308	8.8	21.7	915.8	Land
9/04/92	N	839	3.5	19.7	164.2	Land
9/05/92	D	446	6.2	27.6	432.0	Land
9/13/92	D	605	7.1	25.2	457.9	Land
9/14/94	N	770	5.0	22.8	172.8	Land
9/18/92	D	475	8.6	20.7	518.4	Land

11.5–24.7, 24.7–36.5, 36.5–50.0, 50.0–80.0, 80–125, and >125 μm in diameter. These size ranges were selected to overlap the cut-size intervals of the WRAC. The image processing program was used to isolate and identify the particles of interest. The system defined and isolated single particles from the background and quantified the particle size. At least 10 particles were counted in each size range, and the area counted was recorded. In order to assure that a representative distribution of particles were counted by image analysis, multiple areas were counted and compared. The particles were found to be uniformly distributed on the Myler strips.

Hourly observations of wind speed were used to estimate Reynolds number and friction velocity, V^*, which is determined by

$$U = \frac{V^*}{k}\ln\left(\frac{z + Z_O}{Z_O}\right), \qquad [12]$$

where U is the measured average wind speed, k is Von Karman's constant approximately equal to 0.4, z is the measured height above deposition surface, and Z_O is the aerodynamic roughness height (0.001 cm for smooth deposition surface (Arya 1988)).

DEVELOPMENT OF THE DEPOSITION VELOCITY MODEL

Particles in the atmosphere are deposited by sedimentation (gravitational settling), inertial motion, and diffusion. It is expected that supermicron particles will be deposited by sedimentation and inertial motion, while submicron particles will be deposited by sedimentation and diffusion. Therefore the deposition velocity (V_d) can be approximated by

$$V_d = V_{\mathrm{st}} + V_{di} + V_{dd}, \qquad [13]$$

where V_{st} is the particle settling velocity (Stokes), V_{di} is the particle inertial deposition velocity, and V_{dd} is the particle Brownian diffusion deposition.

Table 2
Measured data for Chicago site independent samples

Sample ID	Sampling time (min)	Avg. wind speed (m/s)	Average temperature (C)	Deposition flux (mg/m2-day)	Avg. wind direction
7/17–23, 94	5135	3.02	25.88	156.3	land/lake
9/14–15, 94	1448	3.98	30.74	423.5	land
9/29–10/6, 94*	3114	3.07	17.92	189.1	lake/land
10/28–29, 94	1124	5.38	15.82	1301.9	land
11/7–11, 94	1480	4.42	11.44	275.6	lake/land
7/7, 8, 10, 95	1222	4.6	24.6	191.2	lake/land
7/11–7/13, 95	1783	4.6	33.4	198.7	land
7/14, 15, 95	1727	4.54	33.81	509.4	land
7/18, 21, 22, 95	1406	3.38	26.54	193.3	lake
7/26–7/29, 95	1973	3.35	28.4	181.8	land/lake
9/11–9/13, 95	1827	3.91	23.5	330.4	land
9/14–9/15, 95	1226	3.62	22.5	232.67	land
9/16–9/18, 95	1327	5.89	20	268.6	land
9/23–9/25, 95	1769	5.75	15.33	145.7	lake

*9/29, 30–10/3–6, 94.

Dimensionless inertial and Brownian diffusion deposition velocities can be obtained as follows:

$$V_{di}^{+} = \frac{V_{di}}{V^*}, \quad V_{dd}^{+} = \frac{V_{dd}}{V^*}, \tag{14}$$

where V^* is the friction velocity (Equation (12))

$$V_d = V_{di} + V_{dd},$$
$$V_d^{+} = V_{di}^{+} + V_{dd}^{+},$$
$$V_d^{+} = \frac{V_d - V_{\mathrm{st}}}{V^*}.$$

The Stokes settling velocity (V_{st}) is given by

$$V_{\mathrm{st}} = \frac{C_c \rho_p g d_P^2}{18\mu}, \tag{15}$$

where ρ_p is the density of the particle, g is the acceleration due to gravity, μ is the absolute viscosity of fluid, d_p is the particle physical diameter, and C_c is the Cunningham slip correction factor.

For large particles ($d_{pa} > 1\ \mu m$), the Brownian diffusion deposition velocity (V_{dd}) is negligible and

$$V_d^{+} = \frac{V_{di}}{V^*} = V_{di}^{+}. \tag{16}$$

This analysis will be used in the model development and the subsequent sensitivity analysis of the model.

Determination of Inertial Deposition Velocity (V_{di}) and Brownian Deposition Velocity (V_{dd})

The experimental dimensionless inertial deposition velocities $(V_{di}^{+})_I$ for particles >1 μm in size were calculated and are provided in Table 1. V_{di}^{+} was plotted against flow Reynolds number (Re) and dimensionless relaxation time (τ^{+}) in a three-dimensional plot (Figure 2). Reynolds number is calculated

Table 3
Data summary for samples collected from Chicago-IIT site

Date	Season	Number of samples	Sampling time: Day/night	Sampling time: Term	Sampling time: Range (hrs)	Wind velocity range (m/s)	Temperature range (C)	Flux range (mg/m2-day)	Use
1992	Summer	28*	D/N	Short	4–16	3.3–8.8	6.1–29.4	86.4–1356	Model development
1994	Summer	1	D	Long	86	3.02	25.88	156.3	Independent
1994	Fall	4	D	Long	19–52	3.07–5.38	11.4–30.7	189.1–1301.9	Independent
1995	Summer	9	D	Long	20–33	3.35–5.89	15.3–38.8	146–509	Independent

*20 Samples used for model development.

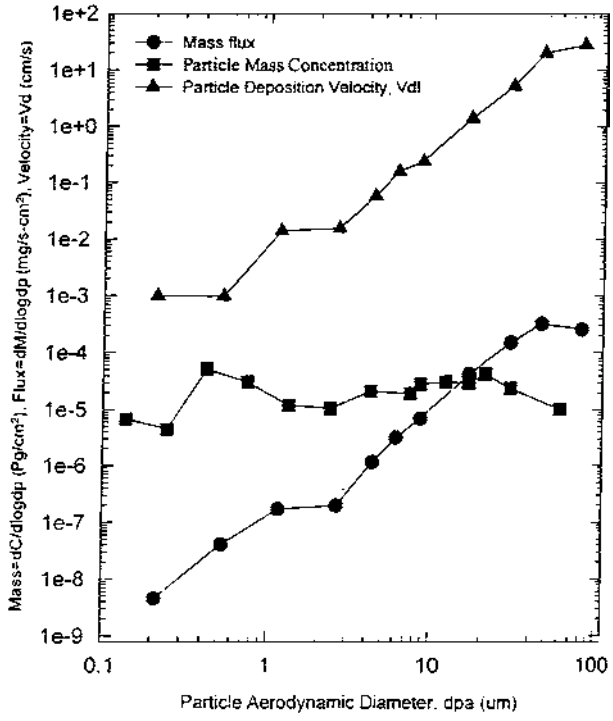

Figure 1. An example of deposition velocities derived from measured ambient particle concentration and count converted mass deposition data.

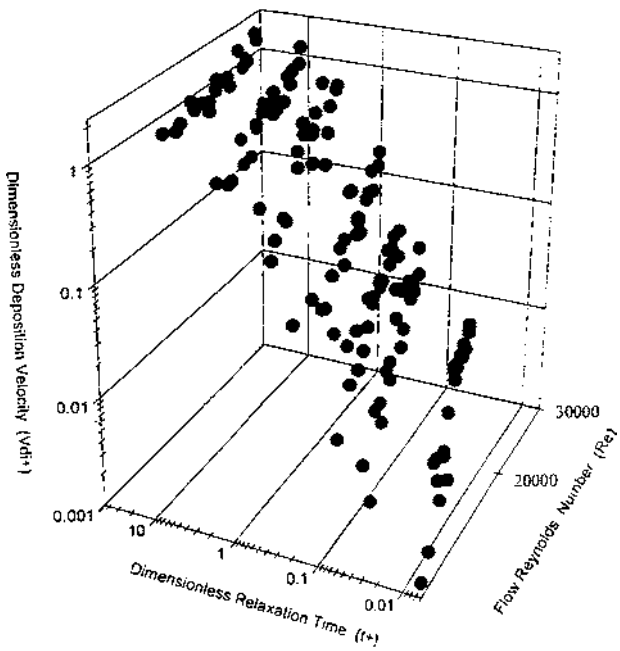

Figure 2. Deposition data collected in Chicago (1992) plotted as nondimensional deposition velocity (V_{di}^{+}) with dimensionless relaxation time (t^{+}) for particles between 1 and 100 μm and atmospheric flow Reynolds number (Re) (Re > 9000).

using the characteristic length of 5 cm, which is the distance from the leading edge to the center of deposition surface, and the wind velocity and kinematic viscosity of the air.

Figure 2 shows an increase of V_{di}^{+} with dimensionless relaxation time (τ^{+}) and flow Reynolds number (Re). The observed increase of dimensionless deposition velocity with flow Reynolds number, for atmospheric data, is of special interest as it shows that the deposition velocity is a function of Reynolds number.

A sigmoid curve (Equation (6)) was fit to the atmospheric data. The coefficients were fit by the least square procedure using the dimensionless atmospheric deposition velocities. The resulting equation is

$$V_{di}^{+} = b_1 e^{-0.5\{(\mathrm{Re}-b_2)/b_3\}^2} + b_4 e^{-0.5\{(\ln_\tau^{+} - \ln b_5)/b_6\}^2}. \qquad [17]$$

The coefficients are $b_1 = 0.024175$, $b_2 = 40{,}300$, $b_3 = 3{,}833.25$, $b_4 = 1.4911534$, $b_5 = 18$, and $b_6 = 1.7$.

The correlation coefficient, R^2, of Equation (17) is 0.83. A statistical analysis (paired t-test) of the data showed that there was no significant difference between dimensionless deposition velocity predicted by Equation (17) and measured values at a 95% confidence interval.

Cleaver and Yates (1975) analyzed the diffusion of small particles onto a smooth wall and found that the dimensionless Brownian deposition velocity takes the form

$$V_{dd}^{+} = 0.084\mathrm{Sc}^{-0.667} = 0.084\left(\frac{V}{D}\right)^{-0.667}. \qquad [18]$$

In applying this equation it is assumed that the Reynolds number term and its coefficients in Equation (19) for inertia also apply to the submicron particle size.

Overall Deposition Velocity Model

Equations (15), (17), and (18) can be used in Equation (13) to provide an overall deposition model as follows:

$$V_d = \frac{C_c(\rho_P - \rho_f)gd_P^2}{18\mu} + V^*\Big\{b_1 e^{-0.5\{(\mathrm{Re}-b_2)/b_3\}^2} + b_4 e^{-0.5\{(\ln_\tau^{+} - \ln b_5)/b_6\}^2} + 0.084\mathrm{Sc}^{-0.667}\Big\}. \qquad [19]$$

The deposition velocities predicted by the ambient model (Equation (19)) are plotted in Figure 3 for Reynolds numbers ranging from 13,000 to 29,000 corresponding to wind velocity and temperature ranges of 2.8 to 9.0 m/s and 14 to 22°C, respectively.

MODEL EVALUATION

Comparison of Model Predictions with Measurements of Atmospheric Deposition Velocities and Sehmel–Hodgson Model Predictions

The 20 sets of atmospheric measurements (Table 1) that were used to develop Equation (19) were grouped into 4 Reynolds

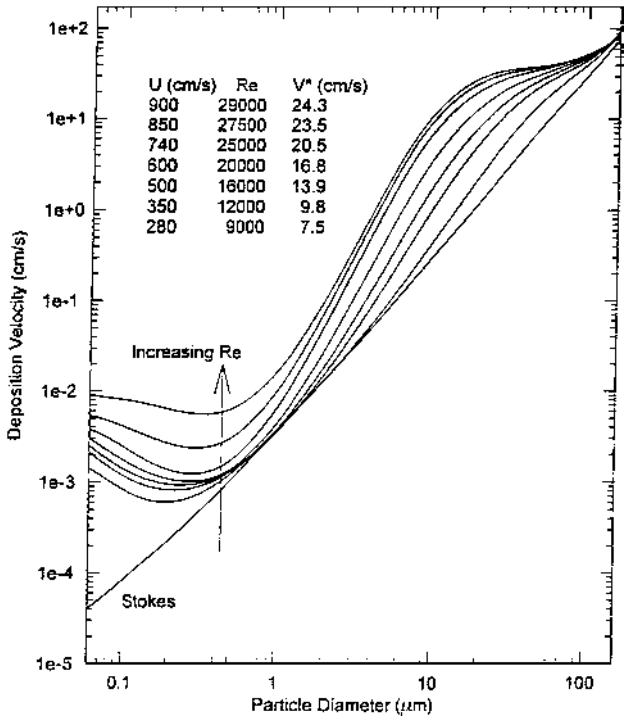

Figure 3. Ambient model calculated particle deposition velocities at a surface roughness of 0.001 (smooth strip on a flat plate).

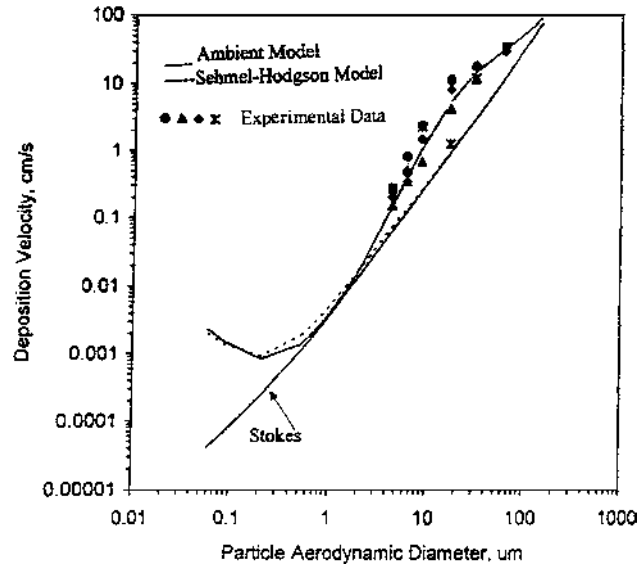

Figure 4. Comparison of experimentally determined deposition velocities (Chicago 1992 data) and velocities predicted with the Sehmel–Hodgson model with ambient deposition model (Reynolds number class II: 13,000 < Re < 17,000).

number classes of 9,000–13,000 (class I), 13,000–17,000 (class II), 17,000–21,000 (class III), and >21,000 (class IV). The average wind velocities for the 4 classes were 3.42, 4.64, 5.82, and 7.87 m/s.

Figure 4 shows a comparison between the experimentally determined deposition velocities for Reynolds number class II and velocities predicted with the ambient deposition velocity model (Equation (19); an example for the Reynolds number classes) for particle sizes between 4 and 100 μm. A comparison between velocities predicted by Sehmel–Hodgson's model to velocities predicted by the ambient model for particle sizes between 0.06 and 4 μm are also shown in Figure 4. For the 20 samples, correlation coefficients (R^2) between measured and modeled deposition velocities for particle size range 4–100 μm were 0.99, 0.99, 0.99, and 0.98 for class I, II, III, and IV, respectively. For particles in the size range 0.06–4 μm, the correlation coefficients (R^2) between predicted velocities by the ambient model (Equation (19)) and the Sehmel–Hodgson wind tunnel model were 0.99, 0.99, 0.99, and 0.98 for class I, II, III, and IV, respectively.

Fourteen atmospheric samples were available (Table 2) as an independent data set not used in the original model development for comparison with the model. Correlation coefficients (R^2) between experimental data and the ambient model predicted velocities for particle size range 4–100 μm were 0.82, 0.86, and 0.93, for class I, II, and III, respectively. For particle size range 0.06–4 μm, the correlation coefficients (R^2) between velocities predicted by the ambient model and the Sehmel–Hodgson wind tunnel model for the three classes were 0.99, 0.99, and 0.99.

Comparison of the Performance of the Ambient Model to the Sehmel–Hodgson Model Using Deposition Velocity Predictions and Experimental Data

Table 4 provides a comparison of the ambient model to the Sehmel–Hodgson model for particle sizes between 4 and 100 μm. In the table, the predicted particle deposition velocities are compared to experimental deposition velocities. Considering the dependent data, Table 4 indicates that for the ambient model the correlation coefficient R^2 remains almost constant at 0.99, while for the Sehmel–Hodgson model an increase in Re is accompanied by a substantial decrease of R^2 from 0.97 for Reynolds number class I to 0.78 for Reynolds number class IV. For the independent data set, as Re increases the ambient model performs better than the Sehmel–Hodgson model.

These results demonstrate that the performance of the ambient model and the Sehmel–Hodgson model is the same at low flow Reynolds numbers (when inertial deposition is minimum), but when the Reynolds number increases the ambient model performs better (Lin 1993; Jackson 1997).

MODEL APPLICATION TO THE PREDICTION OF DEPOSITION FLUX

Comparison of Atmospheric Deposition Flux to Model Predicted Flux Using the Ambient Model and the Sehmel–Hodgson Model

The multistep calculation method (Equation (10)) for dry deposition flux was used to model deposition flux for comparison

Table 4
Comparison of experimental deposition velocities with ambient and Sehmel–Hodgson models predicted deposition velocities

Class	Flow Reynolds number (Re)	Chicago, 1992 data (used for model development) R^2		Independent data R^2	
		Ambient model	Sehmel–Hodgson	Ambient model	Sehmel–Hodgson
I	9000–13000	0.9	0.97	0.82	0.81
II	13000–17000	0.99	0.91	0.86	0.79
III	17000–21000	0.99	0.83	0.93	0.83
IV	21000–29000	0.98	0.78	—	—

with measured flux. The ratio of calculated flux to measured flux was determined for each of the 1992 Chicago samples and independent samples (Tables 1 and 2). A statistical analysis of the data showed that there was no significant difference between the ratios (calculated flux/measured flux) for the 1992 Chicago samples used to develop the model and the independent samples at the 95% confidence interval. Therefore the samples were combined in the following analysis.

Figure 5 indicates that the flux calculated with the multistep method (Equation (10)) in combination with the Sehmel–Hodgson model generally underestimated the measured deposition fluxes (average flux ratio = 0.34 ± 0.18) while the ambient deposition velocity model agreed well with the measured deposition fluxes (average flux ratio = 1.05 ± 0.0.45). Figure 6 shows the average ratio (average calculated flux/measured flux) for the 4 flow Reynolds number classes. The average ratio of calculated/measured flux for the Sehmel–Hodgson model decreases with an increase in the Reynolds number. This is expected since the increase of Re is accompanied by an increase of deposition due to inertia, which is not addressed well

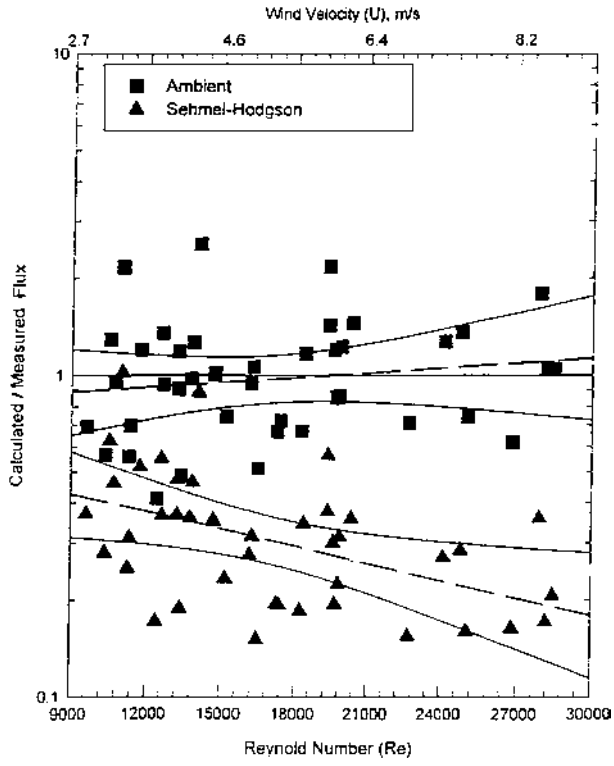

Figure 5. Comparison of measured and modeled flux using the Sehmel–Hodgson model and the ambient model with multiflux calculation method. A linear regression line and 99% confidence intervals are shown.

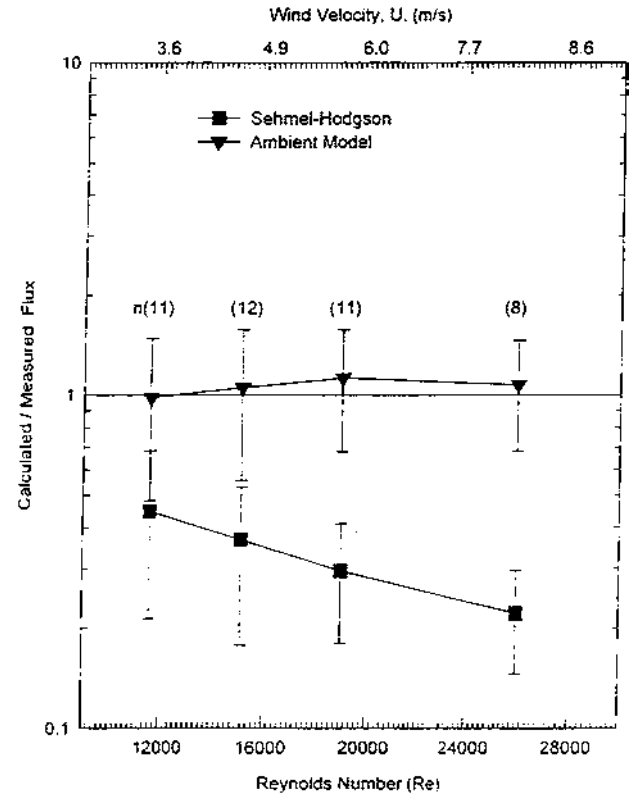

Figure 6. Comparison of average measured and modeled flux using the Sehmel–Hodgson and the ambient model with multiflux calculation method.

by this model (Jackson 1997). The ratio of calculated to measured flux (using Equation (19)) is close to 1 in all 4 Reynolds number classes.

SENSITIVITY ANALYSIS

A sensitivity analysis for calculated deposition velocities has been performed by combining Equation (19) with Equation (14) to obtain dimensionless deposition velocity (V_d^+) as a function of τ^+, Re, and Sc (Figure 7). This figure can be subdivided into three τ^+ ranges.

$\tau^+ > 0.2$ Corresponding to $d_{pa} > 8\,\mu m$. For large particles, the dimensionless deposition velocity (V_d^+) increases rapidly with τ^+ but is independent of the Reynolds number. When τ^+ exceeds 10 ($d_p > 50\ \mu$m), the particles are less able to react to changes produced by turbulent flow until finally the deposition velocity becomes independent of the inertia effects and there is no longer an increase in dimensionless deposition velocity with particle size.

$0.005 < \tau^+ < 0.2$ Corresponding to $1 < d_{pa} < 8\,\mu m$. This is an intermediate size range in which the dimensionless deposition velocity (V_d^+) is a function of dimensionless relaxation time (τ^+) and flow Reynolds number (Re). The observation that deposition is controlled by Re and τ^+ in this size range has also been made by Muyshondt et al. 1996.

$\tau^+ < 0.005$ Corresponding to Particle Diameter $d_{pa} < 1\,\mu m$. For small particles, there is an increase in dimensionless deposition velocity (V_d^+) with Reynolds number (Re). The observed constant dimensionless deposition velocity (V_d^+) (for higher Re number) over a range of dimensionless relaxation time (τ^+) at a constant Reynolds number indicates that the deposition velocity is controlled by factors other than τ^+. The increase of V_d^+ with decreasing τ^+(which varies proportionally with d_{pa}^2) observed for low Reynolds numbers is caused by an increase in the Brownian diffusion coefficient (decrease in Sc; Equations (2), (18), and (19)) with a decrease in particle diameter. Increase of V_d^+ with the decrease of τ^+ is not obvious for higher Re, since the Brownian diffusion contribution is overshadowed by the Re term contribution. The dimensionless deposition velocity for particles with a diameter <1 μm is controlled by Schmidt number and Reynolds number.

Deposition Velocity Model Based on Dimensionless Relaxation Time for Large Particles ($d_{pa} > 8\ \mu$m)

Based on the observation that the dimensionless deposition velocity for the large particle size range ($d_{pa} > 8\ \mu$m) is a function of τ^+ only (Figure 7), the Re number and Sc number terms can be eliminated from Equation (19):

$$V_d = \frac{C_c(\rho_P - \rho_f)gd_P^2}{18^\mu} + V^*\left\{b_4 e^{-0.5\{(\ln\tau^+ - \ln b_5)/b_6\}^2}\right\},$$
$$b_4 = 1.4911534, \quad b_5 = 18, \quad b_6 = 1.7. \qquad [20]$$

The dimensionless deposition velocity (V_d^+) obtained from Equation (20) is plotted against dimensionless relaxation time (τ^+) together with experimental data for large particles ($d_{pa} >$ 8 μm) in Figure 8. The correlation coefficient R^2 is 0.78.

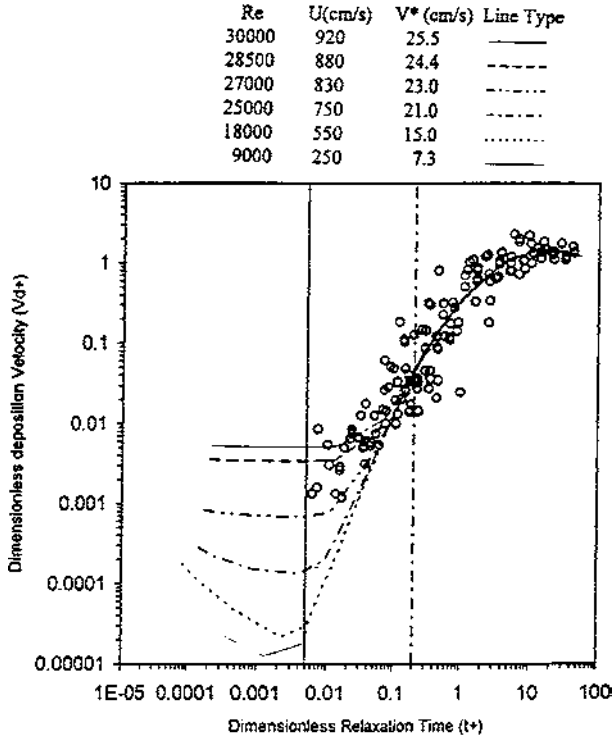

Figure 7. Sensitivity analysis of dimensionless relaxation time, Schmidt number, and flow Reynolds number. Experimental data are shown.

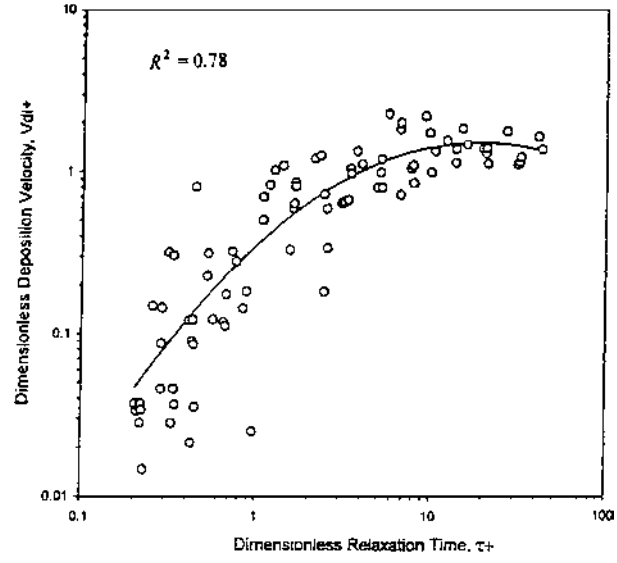

Figure 8. Dimensionless deposition velocity prediction by reduced model using τ^+ term only, and atmospheric experimental data.

Because particles >10 μm in diameter are responsible for the majority of the deposition flux (Davidson et al. 1985; Noll and Fang 1989; Dulac et al. 1989; Holsen and Noll 1992), Equation (20) may be used for calculation of deposition flux under most conditions. When Equations (19) and (20) are used with Equation (10) to predict deposition flux, they produce nearly identical results. The relationship between the fluxes predicted by using Equation (19) (Y) and Equation (20) (X) is $Y = 1.00003X + 134 \times 10^{-5}$ and the correlation coefficient (R^2) between the predicted fluxes using the two equations is 0.99. The reduced model (Equation (20)) is especially useful in the atmospheric environment as it does not depend on Re, which requires an input of characteristic length (L), which varies in the natural environment.

CONCLUSIONS

A. A model for atmospheric deposition has been developed. The model uses a sigmoid curve to correlate dimensionless inertial deposition velocity (V_{di}^+) with dimensionless particle relaxation time (τ^+) and flow Reynolds number (Re). The model is based on
   1) a sigmoid model for deposition in vertical pipe,
   2) atmospheric samples which were used to determine $(V_{di}^+)_I$ for a particle size of range 1–100 μm.

B. Using the multistep flux calculation method, the ambient model generated flux predictions that agreed well with atmospheric measurements. The performance of the ambient deposition velocity model has been compared to the Sehmel–Hodgson model by calculating the ratio (average calculated flux/measured flux). The performance of the ambient model is better than the Sehmel–Hodgson model.

C. A sensitivity analysis for the ambient model has revealed 3 size ranges of model application based on particle diameter. Of the 3 physical parameters (τ^+, Re, Sc) used in the model, not more than 2 parameters control the deposition in any one of these size ranges. Based on this analysis, a reduced deposition model for $d_{pa} > 8$ μm, which is a function of V_{st}, V^*, τ^+ only, has been developed.

D. Data used to develop the model were collected at only one location. Data from other locations is required to extend the applicability of the model. The ambient data were collected using 2 impactors and the deposition data was collected using a smooth surrogate surface that will provide results that are different than deposition to natural surfaces.

REFERENCES

Arya, S. P. (1988). *Introduction to MicroMeteorology*, Academic Press.

Chamberlain, A. C. (1960). In *Aerodynamic Capture of Particles*, Richardson, E. G., Editor, Pergamon Press, New York, pp. 63–88.

Cleaver, J. W., and Yates, B. (1975). A Sublayer Model for the Deposition of Particles from a Turbulent Flow, *Chem. Eng. Sci.* 30:983–992.

Davidson, C. I., Lindberg, S. E., Schmidt, J. A., Cartwright, L. G., and Landis, L. R. (1985). Dry Deposition of Sulphate onto Surrogate Surface, *J. Geophys. Res.* 90:2123–2130.

Dulac, F., Buat-Menard, P., Ezat, U., Melki, S., and Bergametti, G. (1989). Atmospheric Input of Trace Metals to the Western Mediterranean: Uncertainties in Modeling Dry Deposition for Cascade Impactor Data, *Tellus* 41B:362–378.

Friedlander, S. K., and Johnstone, H. F. (1957). Deposition of Suspended Particles from Turbulent Gas Stream, *Ind. Eng. Chem.* 49:1151.

Graseby Andersen Instruments, Inc. (1985). *Operating Manual for Andersen 1 ACFM Non-Viable Ambient Particle Sizing Samplers*, Atlanta, GA.

Holsen, T. M., and Noll, K. E. (1992). Dry Deposition of Atmospheric Particles: Application of Current Models to Ambient Data, *Environ. Sci. Technol.* 25:1807–1815.

Jackson, M. M. (1997). Modeling Atmospheric Particle Deposition, Ph.D. thesis, Illinois Institute of Technology, Chicago, IL.

Kline, S. J., Reynolds, W. C., Schraub, F. A., and Runstadler, P. W. (1967). The Structure of Turbulent Boundary Layers, *J. Fluid Mech.* 30:741–773.

Lin, J., Fang, G., Holsen, T. M., and Noll, K. E. (1993). A Comparison of Dry Deposition Modeled from Size Distribution Data and Measured with a Smooth Surface for Total Particle Mass, Lead, and Calcium in Chicago, *Atmospheric Environment* 15:2639–2646.

Lin, J. J., Noll, K. E., and Holsen, T. M. (1994). Dry Deposition Velocities as a Function of Particle Size in the Ambient Atmosphere, *J. Aerosol Sci.* 20:239–252.

Liu, B. Y. H., and Agarwal, J. K. (1974). Experimental Observation of Aerosol Deposition in Turbulent Flow, *J. Aerosol Sci.* 5:145–155.

Liu, B. Y. H., and Ilori, T. A. (1974). Aerosol Deposition in Turbulent Pipe Flow, *Environ. Sci. Technol.* 8:351–356.

McCready, D. I. (1986). Wind Tunnel Modeling of Small Particle Deposition, *Aerosol Sci. Technol.* 5:301–312.

Muyshondt, A., Arnand, N. K., and McFarland, R. M. (1996). Turbulent Deposition of Aerosols Particles in Large Transport Tubes, *J. Aerosol Sci.* 24:107–116.

Noll, K. E., and Fang, K. Y. (1986). Proc. A Rotary Impactor for Size Selective Sampling of Atmospheric Coarse Particles, *Air Pollution Control Association*. 79th Annual Meeting, Minneapolis, MN, June 22–27.

Noll, K. E., Fang, K. Y., and Watkins, L. A. (1988). Characterization of the Deposition of Particle from the Atmosphere to a Flat Plate, *Atmos. Environ.* 22:1461–1468.

Noll, K. E., and Fang, K. Y. P. (1989). Development of a Dry Deposition Model for Atmospheric Coarse Particles, *Atmos. Environ.* 23:585–594.

Olympus. (1990). *Visualizer PCX Conversion Utility*, Scott Data, Inc., Tonka Bay, MN.

Owen, P. R. (1969). Pneumatic Transport, *J. Fluid Mech.* 39:407–432.

Peters, K., and Eiden, R. (1992). Modeling the Dry Deposition Velocity of Aerosol Particles to a Spruce Forest, *Atmos. Environ.* 26A:2555–2564.

Sehmel, G. A. (1970). Particle Deposition from Turbulent Flow, *J. Geophys. Res.* 75:1766–1781.

Sehmel, G. A. (1971). Particle Diffusivities and Deposition Velocities over a Horizontal Smooth Surface, *J. Collid Interface Sci.* 37:891–906.

Sehmel, G. A. (1973). Particle Eddy Diffusivities and Deposition Velocities for Isothermal Flow and Smooth Surfaces, *Atmos. Environ.* 4:125–138.

Sehmel, G. A., and Hodgson, W. H. (1978). A Model for Predicting Dry Deposition of Particles and Gases to Environmental Surfaces, *DOE Report PNL-SA-6721*, Pacific Northwest Laboratory, Richland, WA.

Slinn, S. A., and Slinn, W. G. N. (1980). Predictions for Particle Deposition on Natural Waters, *Atmos. Environ.* 12:2055–2087.

Tennekes, H., and Lumley, J. L. (1998). *A First Course in Turbulence*, MIT Press, Cambridge, MA.

Wu, H. Y., Davidson, C. I., Dolske, A. D., and Sherwood, S. I. (1992). Dry Deposition of Atmospheric Contaminants: The Relative Importance of Aerodynamic, Boundary Layer, and Surface Resistance, *Aerosol Sci. Technol.* 16:65–81.